PCCP

Check for updates

Surface core level BE shifts for CaO(100): insights into physical origins†

Paul S. Bagus, [ID] [a] Connie J. Nelin,[b] Sergey V. Levchenko,‡[c] Xunhua Zhao,§[c] Earl M. Davis, [ID] [d] Helmut Kuhlenbeck[d] and Hans-Joachim Freund[d]

The relationship between the electronic structure of CaO and the binding energy, BE, shifts between surface and bulk atoms is examined and the physical origins of these shifts are established. Furthermore, the contribution of covalent mixing to the interaction, including the energetic importance, is investigated and found to be small. In particular, the small shift between surface and bulk O(1s) BEs is shown to originate from changes in the polarizable charge distribution of surface O anions. This relationship, which is relevant for the catalytic properties of CaO, follows because the BE shifts are dominated by initial state contributions and the relaxation in response to the core-ionization is similar for bulk and surface. In order to explain the dominance of initial state effects for the BE shifts, the relaxation is decomposed into atomic and extra-atomic contributions. The bonding and the core-level BE shifts have been studied using cluster models of CaO with Hartree–Fock wavefunctions. The theoretical shifts are compared with X-ray photoelectron spectroscopy measurements where both angular resolution and incident photon energy have been used to distinguish surface and bulk ionization.

I. Introduction

The difference of the binding energies, BEs, in the X-Ray photoemission spectroscopy, XPS, spectra of core levels of atoms in the bulk and at the surface of solids, the surface core level shift, SCLS, has been extensively studied for metal surfaces. The different approaches to the interpretation of the significance of the SCLS have been reviewed by Egelhof[1] and by Bagus *et al.*[2] The situation is quite different for the SCLS of oxide surfaces; in contrast to the wealth of information available for metal surfaces, our previous SCLS study of MgO(100)[3] is the only such study available for oxide surfaces. This is surprising since surface core level shifts are intimately correlated with the electronic properties of surface atoms and with their geometrical arrangement, both of which determine the catalytic properties of the surface under investigation.

[a] *Department of Chemistry, University of North Texas, Denton, Texas 76203-5017, USA. E-mail: bagus@unt.edu*
[b] *6008 Maury's Trail, Austin, Texas 78730, USA*
[c] *Abteilung Theorie, Fritz-Haber-Institut der Max-Planck-Gesellschaft, Faradayweg 4-6, D-14195 Berlin, Germany*
[d] *Abteilung Chemische Physik, Fritz-Haber-Institut der Max-Planck-Gesellschaft, Faradayweg 4-6, D-14195 Berlin, Germany*
† Electronic supplementary information (ESI) available. See DOI: 10.1039/c9cp04847b
‡ Current address: Skolkovo Institute of Science and Technology, Skolkovo Innovation Center, 3 Nobel Street, 143026 Moscow, Russia.
§ Current address: Texas Materials Institute and Department of Mechanical Engineering, The University of Texas at Austin, Austin, Texas 78712, USA.

The present work extends our earlier work on the SCLS of MgO to another oxide CaO in order to demonstrate the generality of the mechanisms reported for MgO. Furthermore, careful analyses are made to obtain quantitative information about the extent and the energetic importance of the covalent character of CaO.

If the bulk and surface atoms of an oxide are considered to be ideal ions, the difference of the Madelung potentials of the bulk and surface atoms will give the sign and magnitude of the SCLS. In an octahedral oxide, a bulk ion has 6 nearest counter ion neighbors, whereas a surface ion has only 5 such neighbors. Therefore, the magnitude of the Madelung potential for surface ions will be smaller than for bulk ions. As the Madelung potential raises anion and lowers cation core-level BE's, the surface anion and cation core-level BE's will be lower and higher than in the bulk, respectively.[3] For cubic oxides with lattice constant $\sim$4–5 Å, as for MgO or CaO, the magnitude of the Madelung potential at the surface is different from that in the bulk by $\sim$1 volt. This would certainly lead to an observable BE shift between surface and bulk ions.

In our previous experimental and theoretical study of the SCLS of MgO[3] which is an ideal ionic insulator,[3,4] it was found that the Mg(2p) SCLS is close to the difference of the surface and bulk Madelung potentials. On the other hand, the SCLS of O(1s) was $\sim$0 indicating that other electronic effects must cancel out the difference in the O surface and bulk Madelung potentials. Analysis revealed that the charge distribution of a surface Mg^{2+} is not very different from that of a bulk Mg^{2+}. On the other hand, the more diffuse O^{2-} electron charge

This journal is © the Owner Societies 2019

Phys. Chem. Chem. Phys., 2019, **21**, 25431–25438 | 25431

distribution differs more between bulk and surface atoms. The change in the O charge distribution, while small, is sufficient to cancel the contribution of the Madelung potential leading to an SCLS too small to be resolved. An important question concerns the generality of the MgO results for other oxides; in particular for CaO, also an alkaline earth oxide. Since the Ca 3d is a relatively low-lying level, it is possible that its involvement in the CaO interaction, especially for the core-hole states, could lead to important differences with MgO. Indeed, preliminary results for the CaO SCLS obtained with Density Functional Theory, DFT, slab model calculations[5] suggested a very different SCLS for CaO than for MgO; these results motivated our studies of the CaO SCLS using both cluster and DFT methods. The methodological issues comparing and contrasting DFT and Hartree–Fock, HF, methods and slab and cluster models for CaO were reported in an earlier paper.[6] The objectives of the present paper are to accurately determine the origins of the CaO(100) SCLS and to understand the physical and chemical significance of the SCLS in the context of the surface and bulk electronic structure of CaO.

We will use HF wavefunctions, WFs, for cluster models of bulk and surface CaO. We base our analysis of the bulk and surface electronic structure of CaO on the properties of HF cluster WFs because we have developed theoretical methods to analyze these WFs which allow us to establish connections between the electronic structure and features of the XPS; see, for example, ref. 2 and 7. Our methodological study[6] compared the SCLS for CaO obtained with: (1) periodic slab model DFT calculations; (2) DFT calculations for cluster models of CaO, and (3) HF WFs for these cluster models. Provided that a proper treatment of the neutrality of the slab model supercell was used, all these three models gave similar results for the SCLS. The agreement between the DFT and HF cluster results proves that the HF cluster WFs are sufficiently accurate to analyze the physical and chemical effects involved in the core ionization of CaO. Further support for the accuracy of HF WFs for the description of core level ionization also comes from a comparison of HF and DFT BEs for several gas phase molecules.[8] The correctness of the HF cluster model WFs is also supported by the fact that our theoretical SCLS are fully consistent with our XPS measurements. Specific topics addressed in the present paper are: (1) rigorous analysis of the ionic character of the bonding in CaO with quantitative estimates of covalent departures from ideal ionicity. (2) Characterization of the electronic relaxation in response to core ionization which includes a characterization of the nature and importance of the extra-atomic relaxation arising from the environments of the ionized atoms. (3) Establishing the relationship of these electronic properties to the SCLS. And, (4) identifying the extent that surface reconstruction, both relaxation and corrugation, modifies surface core level BEs and the SCLS. Understanding the differences of the surface and bulk electronic structure will make it possible to drawn connections between the observed SCLS and the properties of the material, including their catalytic properties.

The organization of the paper is as follows: in the following section, methodologies, key details of the experimental and theoretical methods are described. In Sections III and IV, the SCLS results from the experimental XPS and the HF cluster model WFs, respectively, are presented. The conclusions are summarized in Section V.

II. Methodologies

A. Details of the experiments

Core level XPS measurements were performed at the UE56/2 PGM 1 beamline at the BESSY II storage ring (HZB Berlin). Well-ordered CaO(100) films with a thickness of approximately 11 nm were prepared on a Pt(100) single crystal. XPS peak fitting was performed using the CASA XPS software.[9] Prior to fitting, a Shirley background[10] was subtracted from the data. The binding energy scale of the spectra was calibrated using the binding energy of the Au $4f_{7/2}$ core level peak of a Au foil attached to the manipulator. Further details of the CaO film preparation are given in the ESI.†

B. Theoretical considerations

Several clusters were considered but only the results for the larger clusters will be presented since the relevant properties have converged for these clusters. The central atom of the cluster is the atom for which the core-level BEs are determined. This atom is surrounded by shells of neighboring anions and cations chosen so that the edge atoms of the cluster are Ca cations rather than O anions. This cluster is then embedded in a set of point charges chosen to represent the Madelung potential of the extended crystal. The edge Ca cations, which are reasonably rigid, compress the charges associated with the O anions and do not allow them to expand toward the point charges.[11] This compression strongly affects the absolute values of the core-level BEs of the central ion.[11] The cluster models of the CaO(100) surface are formed by truncating the cluster models for the bulk. For the Ca BEs, the clusters are point charge embedded CaO_6Ca_{18} and CaO_5Ca_{13} for bulk and surface respectively where the atoms in each shell are given separately; for the O BEs, the clusters are point charge embedded $OCa_6O_{18}Ca_{38}$, bulk, and $OCa_5O_{13}Ca_{25}$, surface. The clusters are shown in Fig. 1 with the atoms explicitly included shown as large spheres and representative point charges shown as small spheres. For some cases, surface relaxation and corrugation were taken into account in order to be able to estimate their effect for the SCLS. Further details of the clusters are given in the ESI.†

The initial state configuration for all cluster models is closed shell. The core ions have an electron removed from a localized orbital on either Ca or O. Details of the localization are discussed in the ESI.† For the ionization, it is important to distinguish the initial and final state contributions to BEs and to BE shifts, ΔBE,[2] since this distinction is critical to understanding the physical significance of the observed SCLS and their origin in the electronic structure of the oxides. The initial state BEs and ΔBEs are those when the orbitals optimized for the initial state are also used to construct the core-ion WFs. The main contribution to the initial state ΔBE is from the different electrostatic

25432 | *Phys. Chem. Chem. Phys.*, 2019, **21**, 25431–25438

This journal is © the Owner Societies 2019

(a) $OCa_6O_{18}Ca_{38}$

(b) $OCa_5O_{13}Ca_{25}$

(c) CaO_6Ca_{18}
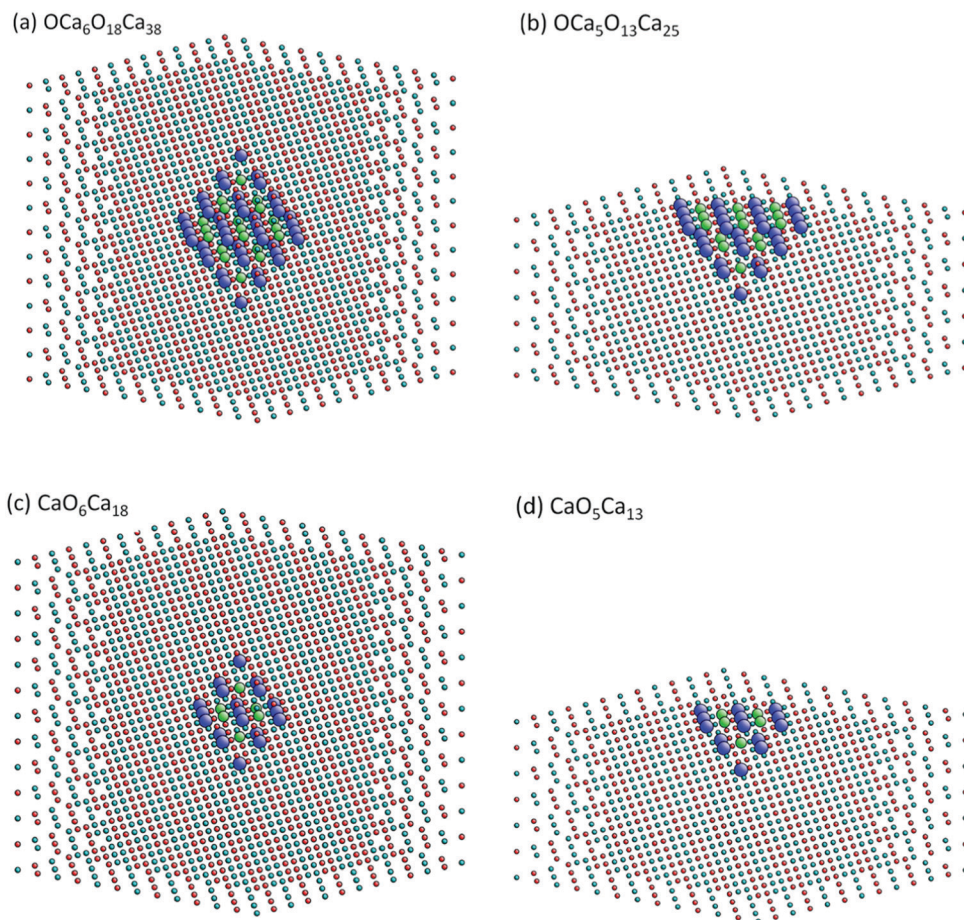
(d) CaO_5Ca_{13}

Fig. 1 Embedded cluster models for the O centered bulk (a) and surface (b) and the Ca centered bulk (c) and surface (d) cases. The atoms used in the cluster are large circles where the oxygen anions are colored green and the Ca cations are colored dark blue (online). The embedding point charges are small circles with red for positive charges and green for negative charges (online).

potentials at the atomic cores of the different ionized atoms; see, for example ref. 2 and 7. The final state contribution to the ΔBE is from the different relaxations in response to the core ionization. When the final state contributions are similar for the core ionization of inequivalent atoms, then the ΔBE reflect the difference of the electrostatic potential at the ionized atoms and provide important chemical information.[2,7] The HF initial state BE for closed shell systems is given by the negative of the orbital energy of the ionized orbital, φ_I, and is referred to as a Koopmans' theorem, KT, BE with $BE(KT) = -\varepsilon_i$. The total BE, including both initial and final state contributions, is the difference of the variationally optimized, self-consistent field, SCF, initial state energy, E(initial), and the variationally optimized energy of the core-ion, E(final), and is referred to as $BE(\Delta SCF) = BE$(final) $- BE$(initial). The relaxation energy, $E(R)$, is the difference of BE(KT) and BE(ΔSCF),

$$E(R) = BE(KT) - BE(\Delta SCF) > 0 \qquad (1)$$

and represents the energy improvement by the response of the orbitals to the presence of the electron hole in the ion.

It is useful to define an extra-atomic relaxation energy, $E_{extra}(R)$, as the difference of the relaxation energy in the cluster model of the material and in the isolated cation or anion fragment,

$$E_{extra}(R) = E(R) - E(R,\text{fragment}). \qquad (2)$$

For a suitable choice of fragment, the extra-atomic relaxation gives the response to the ionization of an atom in the oxide that arises from the presence of the surrounding anions and cations as distinct from the purely atomic response to the ionization. Thus, the quantity $E_{extra}(R)$ provides a novel way to identify the importance of the environment and to understand how the environment of different sites, *e.g.* surface or bulk, can lead to BE shifts. The choice of cation fragment is Ca^{2+} since CaO is an ionic compound. The choice of anion fragment is less clear since O^{2-} does not exist as a stable species and the 2p orbital of O^{2-} will become very diffuse if allowed by the choice of parameters used in the expansion of the orbital.[12] It has been found that the orbitals determined for isolated O^- provide a good characterization of the occupation of anion orbitals in CaO, see Section IV, and the relaxation for the 1s XPS of O^- will be used in eqn (2) for the extra-atomic relaxation of the O 1s XPS of CaO.

For the interpretation of the bonding, including the screening of the core-holes, several methods of analysis of the cluster WFs were used. The occupations of fragment orbitals are determined by projection of the orbitals of isolated Ca^{2+} and O^{2-} on the orbitals of the cluster models.[13] The same orbitals of O^{2-} are used as for the extra-atomic relaxation. This projection has provided a very useful way to estimate the extent of covalency and the degree of ionicity in oxides.[3,14,15] The occupation, $N_P(i)$, given by projection of the ith fragment orbital, $\varphi_i(F)$, is

$$N_P(i) = \sum_j n_j \left| \left\langle \varphi_i(F)\varphi_j \right\rangle \right|^2 \qquad (3)$$

where the sum is over the orbitals φ_j with occupation n_j of the CaO cluster model.[13] The value $N_P(i) \approx 2$ indicates that the fragment orbital is fully occupied in the cluster. Sums over the $N_P(i)$ may be taken to obtain the occupations of atomic shells. Closely related to the projected orbital occupations are the corresponding orbital eigenvalues for the orbitals of the cluster which are most closely related, *i.e.* have the largest overlap, to the fragment orbitals.[3,16,17] It is shown in Section IV that the changes between the surface and bulk O(2p) corresponding orbitals explain the unexpected O 1s SCLS. In the third method of analysis, constraints are placed on the orbital variations following the constrained space orbital variation, CSOV, formalism.[18,19] The energies associated with the constrained variations provide a direct and unique estimate of the energetic importance of the covalent interaction. The application of the CSOV to covalent interactions in oxides is described in ref. 14 the specific use of the CSOV applied to CaO is described in the ESI.†

The point group symmetry of the clusters is O_h for models of the bulk and C_{4v} for models of the surface.[20] The orbitals maintained this symmetry and were spin restricted[21] so that the WFs have the correct spin and spatial symmetries. For the bulk, the O and Ca p orbitals are three-fold degenerate; for the surface, these orbitals are split into a pσ, oriented normal to the surface, and a pπ, oriented parallel to the surface. HF WFs were obtained for the initial states and for the O(1s), Ca(1s), Ca(2s), and Ca(2p) ions. Whether the Ca 3d orbitals, which are low-lying, might play a role in the interaction was investigated but only minor involvement was found. See the ESI† for further details about the WF properties and calculation.

III. Experimental results

Ca 2p photoemission spectra were obtained using various photon energies and electron detection angles in order to distinguish surface components of the core level peak from the bulk component. Some spectra are shown in Fig. 2. The Ca $2p_{3/2}$ peak is best fit by deconvoluting the peak into two Voigt peaks (70% Gaussian), with the main peak at 345.7 eV and another, smaller peak at +0.6 eV higher binding energy. The peak components were constrained to all have the same FWHM within each individual spectrum. Fits of the experimental data in Fig. 2a show that the
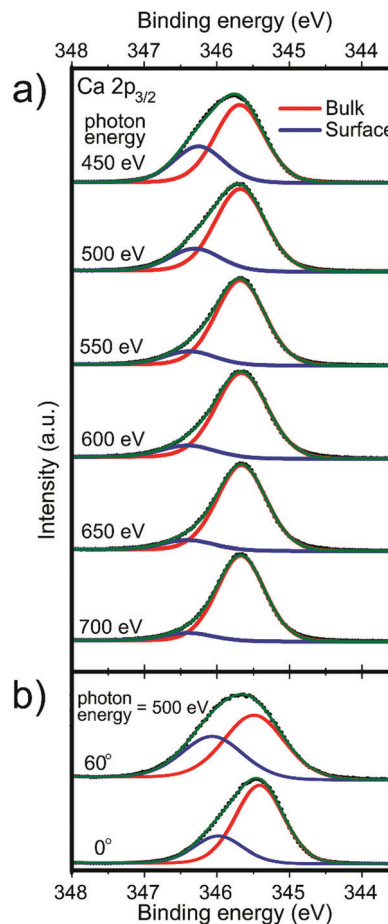

Fig. 2 XPS spectra of the Ca $2p_{3/2}$ core level peak with the surface sensitivity varied by changing (a) the photon energy and (b) the photo-emission angle. Peak heights are normalized for clarity. A decomposition of the total XPS, green online, into bulk, red online, and surface, blue online, contributions is made.

relative intensity of the smaller peak increases from 8% to 31% as the surface sensitivity of the experiment is increased by decreasing the photon energy from 750 eV to 450 eV for spectra recorded at normal emission. Clearly the small peak is the surface Ca $2p_{3/2}$ core level. This conclusion is supported by the data in Fig. 2b which show that the intensity of this peak increases when the experimental surface sensitivity is increased by varying the electron detection angle from 0° (normal emission) to 60° with respect to the surface normal. Since the corresponding O 1s spectra were free of features attributable to hydroxyl groups and since LEED did indicate a well-ordered surface, we conclude that this peak is not affected by either defects or hydroxyls.

O 1s photoemission spectra are shown in Fig. 3 for a variation of the photon energy from 600 to 800 eV. The O 1s peak in each case was fitted with a single Voigt peak as described above. Peaks due to hydroxyl formation were not observed. It was not possible to resolve a surface component from the bulk O 1s peak. Therefore, we conclude that the SCLS for O 1s is less than ~0.1 eV.

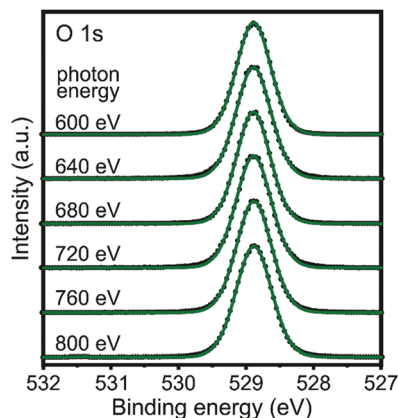Further details on the experimental results are in the ESI.†

25434 | *Phys. Chem. Chem. Phys.,* 2019, **21**, 25431–25438

This journal is © the Owner Societies 2019

Fig. 3 XPS spectra of the O 1s core level taken with photons of different energies. Peak heights are normalized for clarity.

IV. Cluster model results – analysis of the electronic structure & SCLS

The orbital occupations presented in Table 1 are based on projection of the valence orbitals of isolated Ca cations, 3s and 3p, and O anions, 2s and 2p, projected on the orbitals of the bulk and surface cluster models of CaO(100); see Section II and eqn (3). The projections, denoted $N_P(i)$, are given for the initial state where the core orbitals are filled and for the ions where a Ca 2p electron or an O 1s electron have been removed; the Ca 2p ion is for removal of 1/3 of an electron from each of the three 2p orbitals. The Ca orbital projections are made for the Ca centered clusters while the O orbital projections are made for the O centered clusters; see Fig. 2. For the Ca 3s and 3p orbitals, we expect the projections to indicate full occupations with totals of 8 electrons for both the initial state and the 2p ions since the Ca^{2+} cation is rigid and not especially polarizable and this full occupation is shown in Table 1. In particular, the Ca projections show that there is essentially no promotion from the Ca(3p) into the Ca(3d) for the surface Ca cation where this promotion is allowed by symmetry. If the O anions are ideal O^{2-} then the total O 2s and 2p occupations should be 8 for both the initial state and the O 1s ion. For all cases in Table 1, the O

2s and 2p occupation is almost exactly 8 indicating that the O is very nearly an ideal O^{2-} anion and, by extension, that the Ca must be a Ca^{2+} cation. At most only a very small fraction of the O(2p) orbitals, $\sim 1\%$, could be involved with the formation of a covalent bond with Ca. Constrained variations with the CSOV formalism, as described in Section II, allow an estimate of the energetic importance of the covalent bonding to be made for the case of a bulk Ca cation in the initial state without a core ion. The energy improvement by allowing the orbitals of the O anions to mix with the unoccupied orbitals of the Ca^{2+} cation is 0.7 eV where this estimate takes account of limitations of the basis sets used to calculate the WFs. It is important to point out that the 0.7 eV is the estimate for the energetic contribution for the covalent bonding with a single Ca cation.[14] Details of the possible covalent interaction between Ca and O are given in the ESI.† Clearly, the Ca–O interaction is still dominantly ionic and this ionic character of O persists even when an O 1s electron is removed. Although, the projections are similar for bulk and surface O anions, there are subtle differences that will be discussed below.

The persistence of the dominant ionic character of CaO even for the core-level ions has implications for the final state relaxation. The atomic and CaO relaxation energies, $E(R)$, and the extra-atomic relaxation energies, $E_{extra}(R)$ defined in eqn (2), are given in Table 2 for the Ca 2p and O 1s ionizations. There is an uncertainty for the O(1s) $E_{extra}(R)$ since the reference for the atom is taken as O^- which has 5 rather than the 6 electrons shown by the projections to be the O(2p) occupation in CaO; see Table 1 and the discussion in Section IIB. Thus, the O $E_{extra}(R)$ values of 1.8–1.9 eV in Table 2 are upper bounds. It is clear from Table 2 that the extra-atomic relaxation is a small fraction, less than 10%, of the total relaxation. This is consistent with the data in Table 1 which shows that CaO retains its ionic character even when the core-ions are formed, either in the bulk or at the surface. Clearly, the origin of the relatively small extra-atomic relaxation is the polarization of the neighboring ions in response to the change in the charge of the core-ionized atom. The extra-atomic relaxation is larger for the Ca 2p hole than for the O 1s hole for the obvious reason that the nearest O^{2-} neighbors of the Ca core ion are much more polarizable than the nearest Ca^{2+} neighbors of the O core ion. The atomic and extra-atomic relaxations in response to the core holes in CaO can be viewed graphically with the density difference plots which are presented in the ESI.†

If the character of the surface ions remained like those of the bulk ions, one would expect that the $E_{extra}(R)$ would be

Table 1 Orbital occupations, $N_P(i)$, from projections of the outer shell Ca cation, 3s and 3p, and O anion, 2s and 2p, orbitals on the cluster models of CaO. Occupations are given for bulk and surface atoms and for the Ca(2p) and O(1s) ions

Ca	Initial state – $N_P(i)$		2p-Ion – $N_P(i)$	
	Bulk	Surface	Bulk	Surface
3s	2.00	2.00	2.00	2.00
3p	6.00	6.00	6.00	6.00
Total	8.00	8.00	8.00	8.00

O	Initial state – $N_P(i)$		1s-Ion – $N_P(i)$	
	Bulk	Surface	Bulk	Surface
2s	2.00	2.00	2.00	2.00
2p	5.90	5.90	5.93	5.93
Total	7.90	7.90	7.93	7.93

Table 2 Relaxation energies, $E(R)$, for the Ca 2p and O 1s ions of CaO and of the atomic fragments, in eV; extra-atomic $E_{extra}(R)$ are also given

	Ca 2p		O 1s	
Atomic $E(R)$	10.19		20.85	
	Bulk	Surface	Bulk	Surface
CaO $E(R)$	12.74	12.66	22.66	22.76
$E_{extra}(R)$	2.55	2.47	1.81	1.91

This journal is © the Owner Societies 2019

Phys. Chem. Chem. Phys., 2019, **21**, 25431–25438 | **25435**

smaller for the surface ions than for the bulk ions since the surface core ionized atoms have fewer surrounding ions to polarize. For the Ca 2p ions, the surface $E_{extra}(R)$ is, in fact, smaller than the bulk $E_{extra}(R)$ but by less than one would expect given that the surface Ca cations have only 5 O anions as nearest neighbors compared to the 6 for the bulk Ca cations. For the O 1s ions, the surface $E_{extra}(R)$ is actually slightly, $\sim 5\%$, larger than the bulk $E_{extra}(R)$. This indicates that the surface ions, in particular the O^{2-} anions, have a somewhat different electronic distribution than the bulk ions but the $E(R)$ does not provide quantitative information about these differences. However, using corresponding orbitals,[3,16] it is possible to obtain quantitative estimates of the different charge distributions of surface and bulk atoms. The corresponding orbitals between two sets of orbitals are unitary transformations of the occupied orbitals of each set that bring them, as much as possible, into being similar to each other. The criterion for similarity is to find the unitary transformation within a set that leads to the largest overlap between the orbitals of the two sets. The atomic orbitals of either Ca^{2+} or O^- are taken as one of the two sets of orbitals and the orbitals of the bulk and surface CaO clusters as the second set of orbitals. The relevant corresponding orbitals of the CaO clusters are localized on either the bulk or surface atoms and correspond most closely to the atomic Ca or O orbitals. The sizes and shapes of these orbitals, as given by expectation values of $\mathbf{r}$ and r^2, are compared for bulk and surface ions. The coordinates are defined such that z is the normal to the CaO(100) surface and x and y are in the surface plane; the $\langle \mathbf{r} \rangle$ and $\langle r^2 \rangle$ for the corresponding orbitals are taken with respect to the center of the representative bulk or surface atom. By symmetry, all $\langle \mathbf{r} \rangle$ are zero for bulk atoms while for surface atoms only the $\langle z \rangle$ are not zero. In addition, the corresponding orbitals of bulk atoms have spherical symmetry while for surface atoms, the corresponding p orbitals are split into σ and π. For closed shells, where all degenerate orbitals are occupied, the sum of $\langle \mathbf{r}^2 \rangle$ over the orbitals in the shell leads to $\langle x^2 \rangle = \langle y^2 \rangle = \langle z^2 \rangle = \langle r^2 \rangle/3$ for bulk atoms and $\langle x^2 \rangle = \langle y^2 \rangle \neq \langle z^2 \rangle$ for surface atoms. The outermost orbitals of the surface and bulk ions, 2s and 2p for O and 3s and 3p for Ca are of the most interest. Although symmetry separates the s and p orbitals for bulk atoms, for surface atoms s and p can mix in the corresponding orbitals; thus the values of $\langle z \rangle$ and of $\langle r^2 \rangle$ are given for the sums over these orbitals as providing the most meaningful information on the distortion of surface atoms from the essentially spherical symmetry of bulk atoms.

In Table 3, these expectation values for the corresponding orbitals of the initial state cluster WFs are given for the sums over the Ca(3s) + Ca(3p) and over the O(2s) + O(2p) shells. The sizes and shapes of the bulk and surface Ca corresponding orbitals are very similar and this is consistent with the large projected occupations, $N_P(i)$, of these orbitals, see Table 1. There is a small positive $\langle z \rangle$ indicating a slight polarization of the Ca charge toward the vacuum and away from the bulk CaO since there is no compression from the missing O anion above the surface. This polarization also leads to the $\langle z^2 \rangle$ being very slightly larger than the $\langle x^2 \rangle = \langle y^2 \rangle$ for the surface Ca atom.

Table 3 Sizes of the bulk and surface Ca and O ions as given by the sums of $\langle z \rangle$ and $\langle \mathbf{r}^2 \rangle$ for the outer shell corresponding orbitals, 3s and 3p for Ca and 2s and 2p for O; the differences between bulk and surface properties, $\Delta(S-B)$, are also given. The $\langle z \rangle$ are in Å and of $\langle \mathbf{r}^2 \rangle$ in Å^2

		$\langle z \rangle$	$\langle \mathbf{r}^2 \rangle$	$\langle x^2 \rangle = \langle y^2 \rangle$	$\langle z^2 \rangle$
Ca(3s + 3p)	Bulk	0	2.04	0.68	0.68
	Surface	0.02	2.04	0.68	0.68
	$\Delta(S-B)$	0.019	-0.002	-0.002	$+0.004$
O(2s + 2p)	Bulk	0	3.49	1.16	1.16
	Surface	-0.05	3.53	1.19	1.15
	$\Delta(S-B)$	-0.053	$+0.044$	$+0.027$	-0.010

While the changes in size and shape of bulk and surface O anions are small, they are considerably larger than for the Ca cations. The $\langle z \rangle$ shows that the 2s and 2p electrons are drawn toward the bulk since they are attracted toward the Ca cation directly below the surface O. While the magnitude of the $\langle z \rangle$ for the surface O is twice as large as for the surface Ca, the net change, 0.05 Å, is still small compared to the distance of 2.4 Å between the surface and the second layer of CaO. The overall size of the O 2s and 2p electrons, as measured by $\langle r^2 \rangle$ increases by 0.04 Å^2, a 1% change; the lateral size, as measured by $\langle x^2 \rangle$ and $\langle y^2 \rangle$, grows slightly while the vertical size is reduced slightly from the bulk. A further very important consequence, is that, as demonstrated below, the differences between surface and bulk O anion charge distributions, albeit small, are responsible for the anomalous O 1s SCLS.

For the core-level BEs, rather than consider individual BEs, the focus is on the SCLS,

$$SCLS = BE(Surf) - BE(Bulk); \qquad (4)$$

where SCLS > 0 indicates a surface BE greater than bulk and SCLS < 0 a surface BE smaller than bulk. For an CaO(100) surface where no surface reconstruction is allowed, the magnitude of the surface Madelung potential, calculated for the ideal ± 2 ionicities, is 0.8 eV smaller than that for the bulk. Thus, if the Madelung potential is the only reason for the surface core level shifts, the cation SCLS will be $+0.8$ eV and the anion SCLS will be -0.8 eV. The experimental results, Section III, show that the Ca 2p SCLS at $+0.6$ eV has the correct sign and roughly the correct magnitude as predicted from the Madelung potential difference. However, the O 1s SCLS from the XPS measurement is essentially zero and not -0.8 eV. Initial state BE shifts, denoted SCLS(KT), and final state BE shifts including relaxation energies, denoted SCLS(ΔSCF), have been determined for the bulk and surface atoms; see Section IIB for definitions of the KT and ΔSCF BEs. The SCLS(KT) and SCLS(ΔSCF) are presented in Table 4 for several Ca core levels and for O(1s). For the Ca 2p SCLS, the surface 2p BE is for an average ionization of the nearly degenerate surface Ca 2pσ and 2pπ orbitals; see the ESI† for the essentially identical SCLS for surface 2pσ and 2pπ ionization.

Indeed, for all the core-levels, initial state effects dominate the SCLS with changes of 0.1 eV between the SCLS(KT) and the SCLS(ΔSCF), consistent with the data in Table 2 that the extra-atomic relaxation is nearly the same for bulk and surface

25436 | *Phys. Chem. Chem. Phys.*, 2019, **21**, 25431–25438

This journal is © the Owner Societies 2019

Table 4 Initial state and final state SCLS, in eV for the Ca 1s, 2s, and 2p and O 1s levels of CaO

		SCLS(KT)	SCLS(ΔSCF)
Ca	2p(Avg)	0.89	1.01
	2s	0.89	1.00
	1s	0.92	1.00
O	1s	0.15	0.05

atoms. Essentially the same SCLS are found for all the Ca core levels showing that the different surface and bulk initial state environments are the origin of the Ca SCLS. The theoretical cluster model *ab initio* HF SCLS are in qualitative agreement with the XPS measurements. The small theoretical O (1s) SCLS(ΔSCF) is zero within the uncertainty of the XPS measurement. The theoretical Ca(2p) SCLS is large, in agreement with the measurement, but about 50% too large. The SCLS(KT) for the Ca core-levels is $\sim$0.1 eV larger than the 0.8 eV due to the difference of the surface and bulk Madelung potentials but the SCLS(KT) for the O(1s) at +0.15 eV is vastly different from the -0.8 eV due to the difference of the Madelung potentials.

These departures, especially for the O(1s) SCLS, arise from the deformation of the surface O anions from their bulk spherical character and from the small expansion of the O surface charge density. This can be understood by considering the effect of the valence charge density on the KT BEs and SCLSs. The valence charge generates a potential at the nucleus that reduces core-level BEs. Thus, BEs are larger for cations than for neutral atoms or for anions precisely because the potential of the valence electrons acting to reduce the BE is smaller when there are fewer valence electrons in the cation.[7] In a similar way, if the valence charge is expanded, as is the case for the surface O anion, see Table 3, the potential at the nucleus will be reduced and the BEs will be increased. For the bulk and surface O^{2-} anions, a crude approximation for the potential of the eight valence electrons is, in suitable units, $8/r$ where r is the square root of the average 2s and 2p $\langle r^2 \rangle$. Then, the small increase of $\langle r^2 \rangle$ shown in Table 2, for the surface O^{2-} anion compared to the bulk, would lead to an increase in the surface O(1s) BE of greater than 1 eV, completely offsetting the contribution of the Madelung potential that acts to decrease the surface O(1s) BE. The SCLS(KT) for the Ca core levels, $\sim$0.9 eV from Table 4, are $\sim$0.1 eV larger than expected from the difference of the surface and bulk Madelung potentials. While it is possible that the distortion of the surface O valence charge might contribute to this small difference, the contribution of relaxation and reconstruction of the CaO(100) surface also contributes to the change of the SCLS.

Surface relaxation and reconstruction of CaO(100) may contribute to the change of the SCLS from the unreconstructed surface; to estimate the effects that surface relaxation and corrugation have on the SCLS, the CaO clusters have been modified to model these effects. It is noted that the effects of surface relaxation have not been considered previously. For surface relaxation, the surface layer, including the point charges, has been moved closer to the second layer in the embedded CaO_5Ca_{14} and $OCa_5O_{14}Ca_{25}$ clusters by $\Delta z = -0.05$ and -0.11 Å.

Table 5 The Ca(2p) and O(1s) SCLS as the CaO(100) surface layer, relaxation, or the surface atom, corrugation, is moved along the surface normal by Δz; see text. The SCLS are in eV

	Δz in Å	Ca(2p)		O(1s)	
		SCLS(KT)	SCLS(ΔSCF)	SCLS(KT)	SCLS(ΔSCF)
Unrelaxed	0.00	0.89	1.01	0.15	0.05
Relaxed	−0.05	0.81	0.92	0.16	0.06
	−0.11	0.72	0.82	0.19	0.06
Corrugated	−0.05	0.80	0.90	0.15	0.07
	+0.05	0.99	1.12	0.18	0.03

For surface corrugation, only the central surface atom of these clusters has been moved by $\Delta z = +0.05$ and -0.05 Å. These values of Δz for relaxation and corrugation were chosen based on our slab model calculations of CaO(100)[6] where the CaO surface and bulk geometries were optimized. The magnitudes of the Δz are within the ranges found for surface relaxation and corrugation with the slab model. The Ca(2p) and O(1s) SCLS(KT) and SCLS(ΔSCF) for these relaxations and corrugations are given in Table 5 where they are compared with the SCLS for unrelaxed CaO(100). For the Ca(2p) SCLS, both relaxation and corrugation have similar effects on the SCLS; for a change of Δz by -0.05 Å, the Ca SCLS decreases by $\sim$0.10 eV. Furthermore, the SCLS(KT) and SCLS(ΔSCF) changes are parallel indicating that the origin of the changes is an initial state effect arising from a change in the potential at the Ca atom. The SCLSs decrease as the surface atom or layer is brought closer to the second layer and increase when the surface atom is moved away from the surface. These are the directions of changes in the SCLS one would expect from changes in the electrostatic potential due to increasing or decreasing the distance between the central Ca atom and the O anion directly below it in the second layer. It is expected that reconstruction which moves the first layer closer to the second layer will be energetically favorable since reducing the distance between the first and second layers increases the electrostatic attraction between counter ions in these layers. Motion of the surface Ca toward the bulk by 0.1 Å leads to a Ca SCLS(ΔSCF) in better agreement with experiment. For the O(1s) SCLS, the effect of surface reconstruction, both relaxation and corrugation, is much smaller. The difference of the changes of the surface Ca and O BEs due to reconstruction is consistent with the idea that the more polarizable and deformable O^{2-} charge distribution can respond more easily than the more rigid Ca^{2+} to changes in the geometric structure and this will reduce the changes in the O(1s) BEs.

V. Conclusions

This study has extended the understanding of the physical and chemical origins of the SCLS of oxides. It has been found, from both theory and experiment, that the O(1s) SCLS of CaO is small and cannot be resolved from XPS measurements while the Ca(2p) SCLS is large, $\sim$1 eV. The Madelung potentials at the surface cation and anion sites are different by 0.8 eV from the potentials at bulk sites; These differences should lead to a

surface Ca(2p) BE larger by 0.8 eV than the bulk Ca(2p) BE and a surface O(1s) smaller by 0.8 eV than the bulk BE; *i.e.*, to SCLS with $\sim$1 eV magnitude and opposite sign, >0 for Ca and <0 for O. Thus, the small O(1s) SCLS is anomalous. The anomalous behavior has also been found in an earlier study[3] of MgO(100) proving that the small shift of surface O BEs from bulk O BEs is not specific to a particular oxide but is likely to hold for ionic oxides in general. The present study has extended, for CaO, our earlier analyses of the ionic character of MgO to include more detailed analyses of the anion and cation orbital occupations and of the surface and bulk orbital properties. This has included a novel analysis of the orbital screening of the core-hole.

The theory shows that the shifts between surface and bulk BEs, the SCLS, are dominated by initial state effects and, thus, reflect the surface chemistry of the oxide. The origin of the anomalously small O(1s) SCLS is explained as arising from the slight expansion of the polarizable surface O charge distribution and its departure from the spherical symmetry of bulk O anions. Furthermore, the SCLS of other cation core levels besides the Ca(2p) are examined and shown to be very similar to the Ca(2p) SCLS. Thus, the SCLS, in particular for O, reflect the polarization of the CaO surface and are intimately related to the reactivity of this surface. These analyses have made it possible to estimate the small extent of departures in CaO from the ideal ionic, Ca^{2+} and O^{2-}, character. A detailed analysis of the electronic relaxation in response to bulk and surface core ionizations provides new and direct evidence of the primary character of the response as polarization of the anions surrounding the ionized center. It explains why the SCLS are dominated by initial state effects and, thus, reflect the chemistry of the oxide surfaces. The effects of CaO surface reconstruction, including both relaxation and corrugation, on the SCLS have been examined to understand, in particular, the difference in the magnitude of the Ca(2p) SCLS between the theoretical predictions for an unreconstructed CaO(100) surface and the XPS observations. It has been shown that drawing the surface layer atoms closer to the second layer atoms reduces the Ca(2p) SCLS, as expected from electrostatic considerations, but has a much smaller effect on the O(1s) SCLS leaving its value close to zero. This correlation opens the possibility of using measurements of oxide SCLS to obtain information about oxide surface reconstruction.

Conflicts of interest

There are no conflicts to declare.

Acknowledgements

References

1 W. F. Egelhoff, *Surf. Sci. Rep.*, 1987, **6**, 253–415.

2 P. S. Bagus, E. S. Ilton and C. J. Nelin, *Surf. Sci. Rep.*, 2013, **68**, 273.

3 C. J. Nelin, F. Uhl, V. Staemmler, P. S. Bagus, Y. Fujimori, M. Sterrer, H. Kuhlenbeck and H.-J. Freund, *Phys. Chem. Chem. Phys.*, 2014, **16**, 21953–21956.

4 G. Pacchioni, C. Sousa, F. Illas, F. Parmigiani and P. S. Bagus, *Phys. Rev. B: Condens. Matter Mater. Phys.*, 1993, **48**, 11573–11582.

5 Y. Fujimori, X. Zhao, X. Shao, S. V. Levchenko, N. Nilius, M. Sterrer and H.-J. Freund, *J. Phys. Chem. C*, 2016, **120**, 5565–5576.

6 P. S. Bagus, C. J. Nelin, X. Zhao, S. V. Levchenko, E. Davis, X. Weng, F. Späth, C. Papp, H. Kuhlenbeck and H.-J. Freund, *Phys. Rev. B*, 2019, **100**, 115419.

7 P. S. Bagus, E. S. Ilton and C. J. Nelin, *Catal. Lett.*, 2018, **148**, 1785–1802.

8 N. P. Bellafont, F. Illas and P. S. Bagus, *Phys. Chem. Chem. Phys.*, 2015, **17**, 4015.

9 http://www.casaxps.com.

10 D. A. Shirley, *Phys. Rev. B: Solid State*, 1972, **5**, 4709–4714.

11 J. Q. Broughton and P. S. Bagus, *Phys. Rev. B: Condens. Matter Mater. Phys.*, 1987, **36**, 2813–2830.

12 P. S. Bagus and C. W. Bauschlicher, *J. Electron Spectrosc. Relat. Phenom.*, 1980, **20**, 183–190.

13 C. J. Nelin, P. S. Bagus and M. R. Philpott, *J. Chem. Phys.*, 1987, **87**, 2170–2176.

14 P. S. Bagus, C. J. Nelin, D. A. Hrovat and E. S. Ilton, *J. Chem. Phys.*, 2017, **146**, 134706.

15 P. S. Bagus and C. J. Nelin, *J. Electron Spectrosc. Relat. Phenom.*, 2014, **194**, 37.

16 A. T. Amos and G. G. Hall, *Proc. R. Soc. London, Ser. A*, 1961, **263**, 483–493.

17 H. Aagren and P. S. Bagus, *J. Am. Chem. Soc.*, 1985, **107**, 134–137.

18 P. S. Bagus, K. Hermann and C. W. Bauschlicher, Jr., *J. Chem. Phys.*, 1984, **80**, 4378–4386.

19 P. S. Bagus and F. Illas, *J. Chem. Phys.*, 1992, **96**, 8962–8970.

20 S. L. Altmann and P. Herzig, *Point-Group Theory Tables*, Clarendon Press, Oxford, 1994.

21 I. N. Levine, *Quantum Chemistry*, Prentice-Hall, Upper Saddle River, NJ, 2000.

25438 | *Phys. Chem. Chem. Phys.*, 2019, **21**, 25431–25438

This journal is © the Owner Societies 2019